Bicarbonate Binding to the Non-Heme Iron of Photosystem II Investigated by Fourier Transform Infrared Difference Spectroscopy and ^{13}C-Labeled Bicarbonate

Rainer Hienerwadel* and Catherine Berthomieu

CEA Saclay, Section de Bioénergétique, DBCM Bat. 532, 91191 Gif-sur-Yvette, Cedex, France

Received August 17, 1995; Revised Manuscript Received October 17, 1995[⊗]

ABSTRACT: The binding site of the non-heme iron of photosystem II (PS II) is investigated by light-induced Fourier tranform infrared (FTIR) difference spectroscopy on Tris-washed membranes. The non-heme iron is oxidized (Fe^{3+}) in the dark with ferricyanide and reduced (Fe^{2+}) after light-induced charge separation by electron transfer from the semiquinone anion Q_A^-. EPR experiments and IR modes of ferri- and ferrocyanide show that the electron donor side of PS II is reduced in less than 2 s after a flash and that ferricyanide reoxidizes the non-heme iron with a half-time of ≈20 s. Recording FTIR spectra before and 2 s after flash illumination thus results in the Fe^{2+}/Fe^{3+} difference spectrum. This spectrum shows band shifts and intensity changes of IR modes from ligands and neighboring residues of the non-heme iron. The IR modes of bicarbonate are revealed by comparison of Fe^{2+}/Fe^{3+} spectra obtained on PS II membranes with ^{12}C or ^{13}C isotope labeled bicarbonate in H_2O and in ^2H_2O. The ν_{as}(CO) and ν_s(CO) modes of bicarbonate in the Fe^{2+} state are assigned at 1530 ± 10 and 1338 cm^{-1}, respectively. The low frequency of the ν_{as}(CO) mode is taken as experimental evidence that bicarbonate is a ligand of the non-heme iron. Furthermore, the small frequency difference (192 cm^{-1}) between the ν_{as}(CO) and ν_s(CO) modes as compared to even hydrogen-bonded ionic bicarbonate strongly indicates that bicarbonate is a bidentate ligand of the non-heme iron in PS II. Upon iron oxidation, the bicarbonate modes are largely affected. The ν_s(CO) mode is assigned at 1228 cm^{-1}, while the ν_{as}(CO) mode is tentatively assigned at 1658 ± 20 cm^{-1}. The strong up- and downshifts of the ν_{as} and ν_s (CO) modes of bicarbonate upon iron oxidation results in a frequency difference of 430 ± 20 cm^{-1} that is not only explained by the increased charge on the iron but indicates that bicarbonate is a monodentate ligand of the oxidized iron. The sensitivity of the ν_s(CO) mode of bicarbonate to $^1H/^2H$ exchange in both the Fe^{2+} and Fe^{3+} states and the presence in the Fe^{2+} state of a δ(COH) mode at 1258 cm^{-1} confirm that bicarbonate and not carbonate is the iron ligand and further exhibits hydrogen bond(s) with the protein. The ^{13}C isotope-sensitive modes of bicarbonate are not affected by ^{15}N labeling of the PS II membranes. ^{15}N sensitive signals at 1111/1102 and 1094 cm^{-1} are assigned to side chain modes from histidine ligands of the iron. The latter signal is proposed to account for a histidine ligand that deprotonates upon iron oxidation. The involvement of protein peptide groups and side chains in the hydrogen-bond network around the iron is also discussed.

Photosystem II (PS II)[1] is the membrane protein complex of green plants and cyanobacteria that catalyzes the light-driven water oxidation resulting in oxygen evolution. Absorption of a photon leads to charge separation between a chlorophyllic primary donor (P680) and a pheophytin followed by subsequent electron transfer to two plastoquinones, Q_A and then Q_B. A non-heme iron is located between the two plastoquinones. The reaction center (RC) of PS II is made up of two polypeptides D1 and D2 homologous to the L and M subunits of the RC of purple photosynthetic bacteria (Trebst, 1986). The electron transfer steps involving the quinones are very comparable in the two types of organisms, and the quinone environment of PS II can be roughly modeled by the known structure of the bacterial RC. In the bacterial RC, the non-heme iron is found almost equidistant to the two electron acceptor quinones. Four histidines from the polypeptides L and M and a bidentate glutamate (M-Glu232, *Rhodobacter sphaeroides* numbering) provide the iron ligands (Allen et al., 1988; Deisenhofer & Michel, 1989). Four histidines, homologous to those of the bacterial RC, are found in the D1 and D2 polypeptides of PS II which probably coordinate the non-heme iron (Trebst, 1986; Michel & Deisenhofer, 1988). Mössbauer spectra of the non-heme iron in PS II showed the characteristics of a high-spin (S=2) Fe(II) iron coordinated in a similar distorted octahedral arrangement as in the bacterial RC (Diner & Petrouleas, 1987a). Besides these similarities, no residue homologous to M-Glu232 can be identified in the D2 polypeptide sequence of PS II. Instead bicarbonate has been suggested to be responsible for some specific properties of the quinone−iron electron acceptor side of PS II [Wydrzynski & Govindjee, 1975; for reviews see Blubaugh and Govindjee (1988), Diner et al. (1991), and Govindjee and Van Rensen (1993)] since its replacement by formate or other small

* Corresponding author.

[⊗] Abstract published in *Advance ACS Abstracts,* December 1, 1995.

[1] Abbreviations: EPR, electron paramagnetic resonance; FTIR, Fourier transform infrared; IR, infrared; Tris, Tris(hydroxymethyl)-aminomethane; ν_{as} (ν_s), asymmetric (symmetric) stretching vibration; δ, bending vibration; PS II, photosystem II; RC, reaction center; Fe^{2+} (Fe^{3+}), the non-heme iron in its reduced (oxidized) state; P680, chlorophyllic primary electron donor of PS II; Q_A (Q_B), primary (secondary) plastoquinone electron acceptor of PS II; D1, and D2, polypeptides that coordinate the primary reactants of the PS II RC; Tyr $_Z$, tyrosine D1 161, secondary electron donor of PS II; DCMU or diuron, 3-(3,4 dichlorophenyl)-1,1-dimethylurea; 4-MeImH, 4(5)-methylimidazole; 4-MeIm$^-$, 4(5)-methylimidazolate; ImH, imidazole.

0006-2960/95/0434-16288$09.00/0

anions alters several characteristics of the electron acceptor side of PS II. Bicarbonate exchange by formate modifies the EPR spectra of the semiquinone−iron complex (Vermaas & Rutherford, 1984). The presence of bicarbonate determines the electron transfer rates between the quinones (Stemler & Murphy, 1985; Eaton-Rye & Govindjee, 1988). It modifies the binding of herbicides (Vermaas et al., 1982; Wraight, 1985) and determines the midpoint potential of the non-heme iron and its pH dependence (Deligiannakis et al., 1994; Petrouleas et al., 1994). EPR spectroscopy and fluorescence yield relaxation measurements have shown that nitrogen oxide (NO) is a ligand to the non-heme iron and that it competes with bicarbonate, supporting that bicarbonate is also a fully dissociable ligand of the iron (Petrouleas & Diner, 1990; Diner & Petrouleas, 1990). The examination of the Fe^{2+}−NO EPR signals in oriented membranes places the NO ligand at a position approximately homologous to one of those occupied by M-Glu232 in the bacterial RC (Deliagiannakis et al., 1992). However, the binding of bicarbonate has not been directly observed so far and its mode of binding—monodentate or bidentate—is still not determined. Formate/bicarbonate exchange experiments and site-directed mutagenesis also showed that the properties of bicarbonate partly rely on its interactions with protein residues, notably with Lys and Arg side chains (Cao et al., 1991; Diner et al., 1991), and covalent binding of bicarbonate to a Lys side chain forming a carbamate was even not excluded (Diner et al., 1991).

Unlike in the bacterial RC, the non-heme iron in PS II can be oxidized by ferricyanide (Ikegami & Katoh, 1973; Petrouleas & Diner, 1986) and reduced by the primary semiquinone anion Q_A^- on the microsecond time scale (Bowes et al., 1979; Petrouleas & Diner, 1987). The possibility of photoreduction of the non-heme iron in PS II allows the study of its environment by light-induced FTIR difference spectroscopy. With this technique, infrared absorbance changes down to 10^{-5} of the maximum sample absorption are detected, so that insights on the cofactor-protein interactions can be obtained at the molecular level [reviewed in Mäntele, (1993)]. In addition, IR and Raman spectroscopy are the traditional means of ascertaining the binding modes of metal-coordinated carbonates and carboxylates (Nakamoto, 1986; Deacon & Phillips, 1980). A first report of the light-induced Fe^{2+}/Fe^{3+} FTIR difference spectrum has been published by Hienerwadel et al. (1993a). A comparable spectrum has been recently reported by Noguchi & Inoue (1995a). In the present study, we focus on the IR modes of bicarbonate which are identified by comparing difference spectra obtained in Tris-washed PS II membranes in the presence of ^{12}C and ^{13}C isotope-labeled bicarbonate. Spectra obtained with ^{14}N and ^{15}N-labeled PS II membranes are also compared to determine the contributions from the histidine ligand(s) and from amino acids involved in bicarbonate binding.

MATERIALS AND METHODS

Photosystem II-enriched membranes were prepared from spinach according to the method of Berthold et al. (1981) with modifications of Ford and Evans (1983) and stored at −80 °C. Tris washing of the membranes was performed with 0.8 M Tris, pH 8.5, at 0 °C for 30 min, followed by centrifugation and resuspension in buffer A (50 mM Tris, pH 8, 10 mM NaCl, and 5 mM $MgCl_2$). For exchange with ^{13}C labeled bicarbonate, the samples were incubated in a 1 M ^{13}C bicarbonate solution (Euriso-Top, Saclay-France) for 3 h at 0 °C, followed by two successive washing steps in buffer A with 50 mM ^{13}C bicarbonate. ^{15}N labeled spinach was obtained by A. Boussac from spinach cultivated with a liquid medium containing $^{15}NO_3$, $(^{15}NH_4)_2SO_4$ and $Ca(^{15}NO_3)_2$ with 99% ^{15}N as nitrogen sources (Zimmermann et al., 1993).

The IR samples consisted of a PS II membrane pellet sandwiched between two CaF_2 windows (≈6 μm optical path length) in the presence of ferricyanide and were prepared as described by Hienerwadel et al. (1993a). The ferricyanide concentration in the sample was about 10 mM and the chlorophyll concentration was ≈15 mg/mL. The FTIR measurements were performed at 4 °C in H_2O and at 8 °C in ^2H_2O in a thermostated sample holder. The absorption of the samples in the amide I and water absorption region around 1650 cm^{-1} was kept below 0.9 absorbance unit. Illumination of the samples was performed by the broad-band emission of sulforhodamine 101 pumped by a 10-ns pulse of a frequency-doubled Nd−Yag laser (Quantel YG 780−50). FTIR spectra were recorded on a Bruker IFS 88 SX spectrometer. Spectra were obtained by taking 64 scans (corresponding to ≈11 s recording time) before and either 2 or 13 s after a saturating flash. The acquisition duration was chosen to optimize the S/N ratio in respect to the signal decay. The light-induced reactions were cycled with 80 s between flashes for an average of 24 h. Spectra obtained with 2−8 samples were averaged.

CW-EPR spectra were recorded at 278 K or at helium temperature on a Bruker ER 200D X-band spectrometer equipped with an Oxford Instruments cryostat, a HP5350B microwave frequency counter, and a Bruker ER 35 NMR gaussmeter for the detection of the *g*-values. The EPR sample consisted of a fraction of the same pellet as used for the FTIR experiments deposited on a mylar sheet in an EPR tube sealed under helium atmosphere.

RESULTS

Reliable interpretation of a light-induced FTIR difference spectrum depends on the precise characterization of the light-induced reaction that was performed. To study the IR changes induced by the photoreduction of the non-heme iron, we used Tris-washed PS II enriched membranes in the presence of ferricyanide. Only ferricyanide was added to the sample, but the IR absorption spectrum of the sample indicated that 4−5% of ferricyanide was reduced into ferrocyanide in the dark before the experiments (not shown). In these experimental conditions, the light-induced electron transfer is expected to occur as displayed in Figure 1. The non-heme iron is oxidized by ferricyanide in the dark-adapted sample. Light-induced charge separation between P680 and Q_A is followed by the oxidation of $tyrosine_Z$—the electron donor to $P680^+$ (Babcock & Sauer, 1975; Barry & Babcock, 1987)—and by the reduction of the iron in a few microseconds (Bowes et al., 1979; Petrouleas & Diner, 1987). In Tris-washed membranes, ferrocyanide can reduce the donor side of PS II on a millisecond time scale (Dekker et al., 1984). The half-times given in Figure 1 have been determined in the FTIR experimental conditions.

The oxidation state of the iron as well as the reduction kinetics of the electron donor side of PS II were monitored

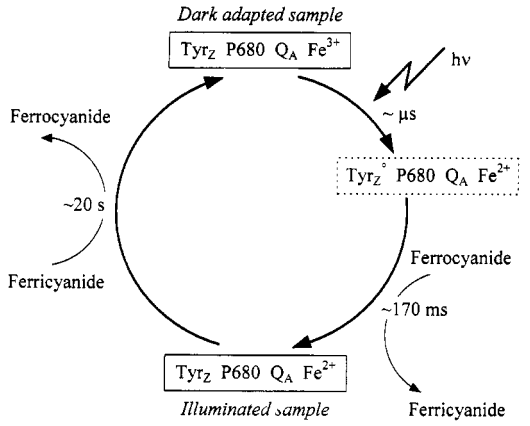

FIGURE 1: Reaction scheme of the light-induced electron transfer in Tris-washed PS II membranes under oxidizing conditions (ferri/ferrocyanide). The half-times are determined for the FTIR experimental conditions.

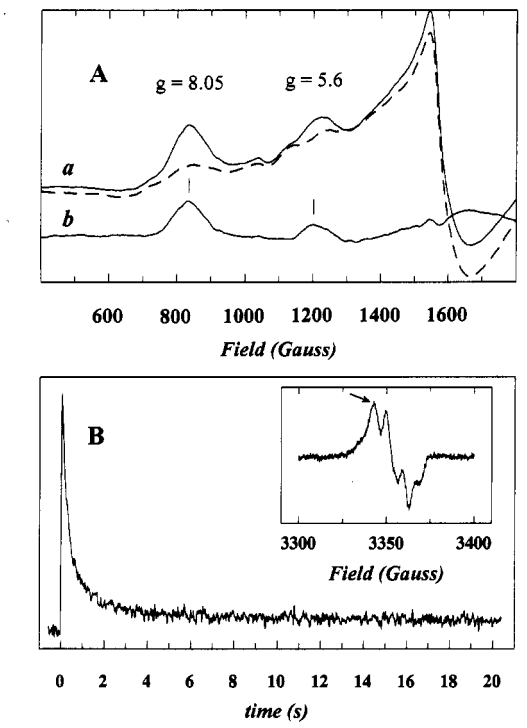

FIGURE 2: (A) EPR spectra of Tris-washed PS II membranes at pH 8 under oxidizing conditions (ferri/ferrocyanide): (a) dark-adapted (solid line) and illuminated (dashed line) sample (after 2-s illumination at 0 °C); (b) dark-adapted *minus* illuminated difference spectrum. Experimental conditions: 4.6 K, microwave power 32 mW, amplitude modulation 32 G, modulation frequency 100 kHz, microwave frequency 9.4 GHz. (B) Reduction kinetics of the Tyr• EPR signal at 278 K induced by laser flash illumination, measured at the low-field maximum of Tyr• EPR signal (arrow in the inset). Experimental conditions: microwave frequency 9.42 GHz, modulation amplitude 6.57 G, microwave power 12.7 mW, time constant 20.48 ms; accumulation of 8 traces with 80 s between flashes. (Inset) Tyr$_D$• EPR signal at 278 K. Experimental conditions: microwave power 12.7 mW, amplitude modulation 2.94 G, modulation frequency 100 kHz, microwave frequency 9.4 GHz.

by EPR in conditions as close as possible to those of the FTIR experiments, i.e., using a fraction of the same PS II membrane pellet deposited on a mylar sheet. The EPR spectrum recorded at 4.6 K of dark-adapted Tris-washed PS II membranes in the presence of ferricyanide shows the characteristic signals at $g = 8.05$ and 5.6 [Figure 2A(a), solid line] of the iron Fe^{3+} (Petrouleas & Diner, 1986). The absence of signal at $g = 6$ indicates that no modification of the iron environment occured during sample preparation (Deligiannakis et al., 1992). The EPR spectrum of the same sample after illumination at 0 °C for 2 s and immediate freezing to 77 K and then to 4.6 K is shown in Figure 2A(a) (dashed line). The subtraction of the EPR spectra recorded before and after illumination (dark-adapted *minus* illuminated spectrum) demonstrates that a large fraction of the iron is photoreduced in these conditions [Figure 2A(b)].

The EPR spectrum recorded at 278 K on the dark-adapted PS II sample (Figure 2B, inset) shows the characteristic signal at $g = 2.0044$ of the stable tyrosine $_D$ radical (Babcock & Sauer, 1973). The decay kinetic of the flash-light-induced tyrosine radical (Tyr^0) was determined by EPR at the same temperature as for the FTIR experiments, i.e., 278 K (Figure 2B). Eighty percent of the photooxidized tyrosine is reduced with a half-time of 170 ms, and the remaining 20% disappears with a half-time of ≈1.3 s. Two seconds after the flash, only a negligible amount of Tyr• is present. The EPR experiments also indicated that no chlorophyll is photooxidized under 1-Hz flash illumination and that cytochrome b559 was already in the low-potential form and oxidized in the dark (not shown).

Two single-beam spectra, dark-adapted and illuminated, were recorded before and after the flash, respectively, on the Tris-washed PS II membranes to calculate the illuminated *minus* dark-adapted FTIR difference spectra. Data acquisition for the illuminated spectrum was started at least 2 s after the flash to minimize contributions of the tyrosine radical. The FTIR difference spectrum in the 1800−1000-cm^{-1} region is displayed in Figure 3A (thick line). For these measurements 50 mM ^{12}C bicarbonate was added to the final buffer. Identical spectra were obtained if no bicarbonate was added during PS II membranes and sample preparation. In the subsequent FTIR difference spectrum, where the illuminated spectrum is recorded 13 s after flash illumination (Figure 3A, thin line), the same signals are present but with reduced amplitudes.

The amplitude decrease of the signals can be correlated with the decrease of the IR signals of ferro- and ferricyanide which are observed in the 2200−1900-cm^{-1} region of the FTIR difference spectra (Figure 4). In this region no protein signals are usually observed. The ν(C≡N) stretching modes of ferri- and ferrocyanide are observed at 2116 and 2040 cm^{-1}, respectively, with an approximately 4 times larger extinction coefficient for ferrocyanide. In the first FTIR difference spectrum with the illuminated spectrum recorded 2 s after the flash (thick line), the positive band at 2116 cm^{-1} and the negative one at 2040 cm^{-1} demonstrate that ferrocyanide was oxidized into ferricyanide after the flash. Time-resolved IR measurements at the ν(C≡N) vibration of ferrocyanide in similar conditions showed that this signal disappears with a half-time of around 100 ms (Hienerwadel, 1993b). In the subsequent difference spectrum (Figure 4, thin line) the amplitudes of the signals are reduced, showing that the initial signals due to ferrocyanide oxidation are progressively canceled by a slow reduction of ferricyanide into ferrocyanide which takes place with a half-time of ≈20 s.

The spectrum displayed in Figure 3B results from the subtraction of the two FTIR difference spectra of Figure 3A after normalization to the amplitude of the ferrocyanide signal in Figure 4 (thick line). This spectrum exhibits an almost

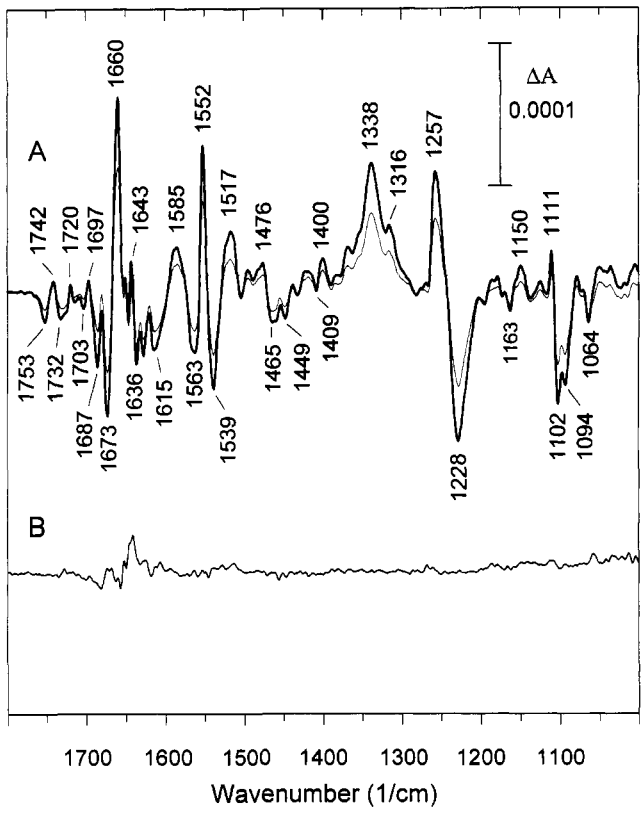

FIGURE 3: (A) FTIR difference spectra (illuminated *minus* dark-adapted) in the 1800−1000-cm^{-1} region obtained on Tris-washed PS II membranes at pH 8 under oxidizing conditions (ferri/ferrocyanide); delay between flash and data accumulation for illuminated spectrum was 2 s (thick line) or 13 s (thin line). (B) Difference spectrum calculated from spectra in panel A after normalization to the amplitude of the ferrocyanide signal at 2040 cm^{-1} of Figure 4 (thick line). The frequencies are given ±1 cm^{-1}, 4-cm^{-1} resolution, ≈350 000 scans.

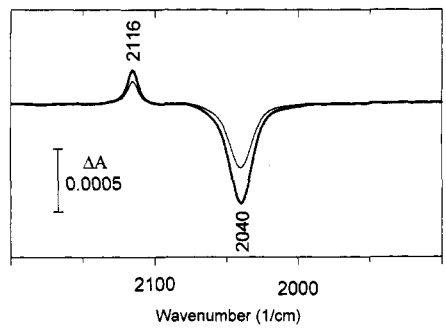

FIGURE 4: The 2200−1900-cm^{-1} region of the FTIR difference spectra of Figure 3A; delay between flash and data accumulation for illuminated spectrum was 2 s (thick line) or 13 s (thin line).

flat line. Small changes in the frequency region around 1650 cm^{-1} are mainly explained by the higher noise level in this region of high sample absorption (amide I and water). We conclude from these observations that all signals in the FTIR spectra correspond to the same light-induced state decaying with a half-time of ≈20 s and that contribution of signals with shorter decay times are negligible. Therefore all signals observed in the 1800−1000-cm^{-1} region result from IR absorption changes from the electron acceptor side of PS II reoxidized by ferricyanide.

The spectra of Figure 3A show no similarities with the Q_A^-/Q_A difference spectra obtained on the same type of spinach PS II membranes (Berthomieu et al., 1990, 1992a). In particular, the strong positive band at 1478 cm^{-1} of the Q_A^-/Q_A difference spectra, tentatively assigned to the ν(C···O) mode of the semiquinone anion, is absent in the spectra of Figure 3A. Additional Q_A^-/Q_A signals were only observed in FTIR difference spectra when the illuminated spectrum was recorded under strong continuous light. Under low-light-intensity continuous illumination, the spectra were identical to those in Figure 3A (not shown). These observations are in agreement with the attribution of the FTIR spectra in Figure 3A to the photoreduction of the non-heme iron or of an electron acceptor located after Q_A. Comparison with results on the bacterial RCs (Breton et al., 1991) and model compounds (Bauscher et al., 1990) suggests that the formation of Q_B^- in PS II should also give rise to a strong ν(C···O) vibration in the region from 1500−1450 cm^{-1}. No signals are observed in the difference spectra of Figure 3A which could account for this mode. The small positive signal at 1476 cm^{-1} disappears in ^2H_2O (Figure 6A) and is downshifted upon ^{15}N labeling (Figure 7A) and cannot be due to a mode of a semiquinone anion. Furthermore, the high concentration of ferricyanide makes a stable Q_B^- over more than 10 s quite unlikely, so that we rule out significant contributions of Q_B^-/Q_B signals to the spectra.

FTIR and EPR control measurements show that the FTIR difference spectra of Figure 3A represent IR changes induced by the photoreduction of the non-heme iron in PS II, and the FTIR difference spectra are thus called the Fe^{2+}/Fe^{3+} spectra. If in some PS II centers the iron is not oxidized prior to the flash, Q_A may be photoreduced but its short lifetime, due to either charge recombination with $Tyr_Z^\bullet$ (Dekker et al., 1984) or to fast reoxidation by ferricyanide, prevents any contribution to the Fe^{2+}/Fe^{3+} spectra. In the 1800−1000-cm^{-1} region, the Fe^{2+}/Fe^{3+} spectra exhibit the vibrational modes of the iron ligands and nearby residues affected by the iron reduction. Negative (positive) bands correspond to the Fe^{3+} (Fe^{2+}) state. To determine the specific contributions of bicarbonate, we have studied the effect of ^{13}C isotope labeling of bicarbonate on the IR spectra recorded in H_2O, ^2H_2O, and with ^{15}N-labeled PS II membranes.

Figure 5A compares the Fe^{2+}/Fe^{3+} FTIR difference spectra obtained at pH 8 in the presence of ^{12}C- (thick line) and of ^{13}C- (thin line) bicarbonate. The spectra are normalized on the negative ferrocyanide band at 2040 cm^{-1}. Only a few signals of the Fe^{2+}/Fe^{3+} spectra are influenced by isotope labeling of bicarbonate. In particular, the spectra are very similar below 1200 cm^{-1} or above 1680 cm^{-1}. Figure 5B shows the result of the subtraction of the Fe^{2+}/Fe^{3+} spectra of Figure 5A and is further denoted ^{12}C *minus* ^{13}C spectrum. This spectrum exhibits only the ^{13}C isotope-sensitive modes of bicarbonate. Positive bands can be assigned either to modes of ^{12}C bicarbonate in the Fe^{2+} state or to modes of ^{13}C bicarbonate in the Fe^{3+} state. Negative bands are due either to modes of ^{12}C bicarbonate in the Fe^{3+} state or to modes of ^{13}C bicarbonate in the Fe^{2+} state. The definitive attribution is made by comparison of the ^{12}C *minus* ^{13}C spectrum with the Fe^{2+}/Fe^{3+} spectra of Figure 5A, and knowing that only frequency downshifts (less than 60 cm^{-1}) are expected for modes of bicarbonate upon ^{13}C labeling in the frequency region from 1800−1000 cm^{-1} (Bernitt et al., 1965; see discussion).

The ^{12}C *minus* ^{13}C spectrum (Figure 5B) exhibits positive bands at 1339 and 1205 cm^{-1} and negative bands at 1305 and 1230 cm^{-1}. The band at 1339 cm^{-1} corresponds to the

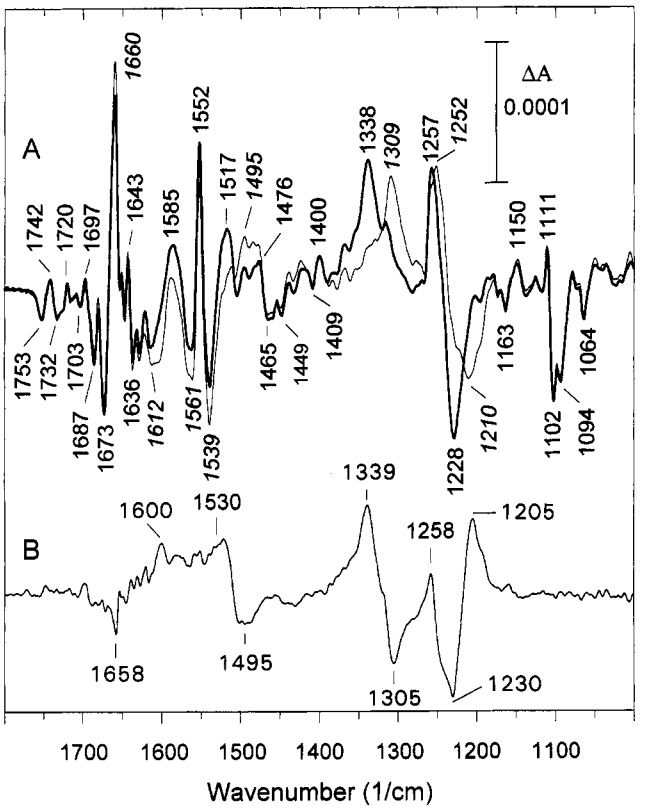

FIGURE 5: (A) Fe^{2+}/Fe^{3+} spectra obtained on Tris-washed PS II membranes at pH 8 with ^{12}C- (thick line) or ^{13}C- (thin line) bicarbonate; spectra are normalized to the same ferrocyanide signal at 2040 cm^{-1} of Figure 4. (B) ^{12}C *minus* ^{13}C spectrum obtained by the difference between spectra in panel A; 4-cm^{-1} resolution, 4 °C, ≈350 000 scans.

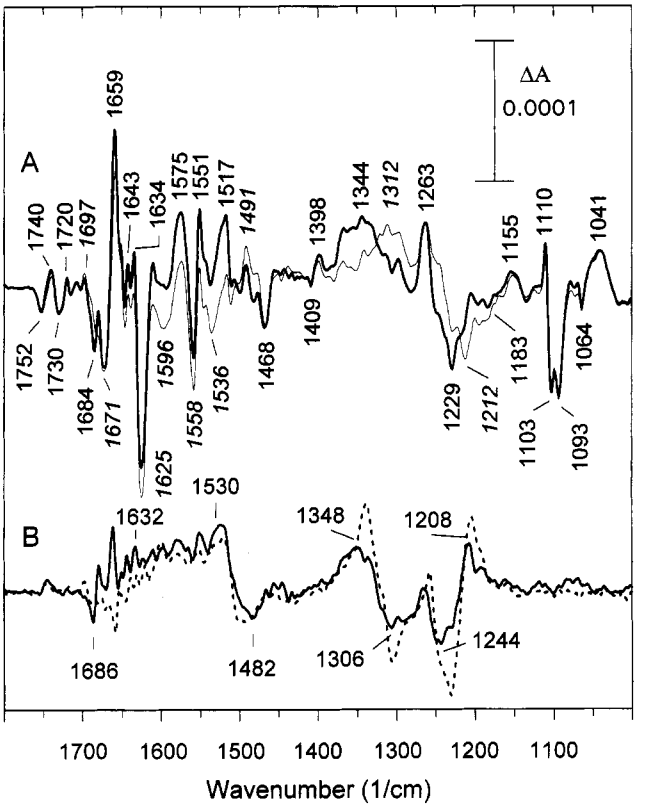

FIGURE 6: (A) Fe^{2+}/Fe^{3+} spectra obtained on Tris-washed PS II membranes at pD 8 in ^2H_2O with ^{12}C- (thick line) or ^{13}C- (thin line) bicarbonate; spectra are normalized as in Figure 5A. (B) ^{12}C *minus* ^{13}C spectrum in ^2H_2O (solid line) and H_2O (dashed line); 4-cm^{-1} resolution, 8 °C, ≈220 000 scans.

positive band observed at 1338 cm^{-1} in the Fe^{2+}/Fe^{3+} spectrum (Figure 5A, thick line). This band clearly shifts down to 1309 cm^{-1} (Figure 5A, thin line) upon bicarbonate ^{13}C labeling. The negative band at 1305 cm^{-1} in the ^{12}C *minus* ^{13}C spectrum (Figure 5B) confirms this assignment. The 1338 and 1309 cm^{-1} bands are therefore assigned to modes of ^{12}C- and ^{13}C-bicarbonate in the Fe^{2+} state, respectively. The positive band at 1205 cm^{-1} and negative one at 1230 cm^{-1} in the ^{12}C *minus* ^{13}C spectrum (Figure 5B) are interpreted as the downshift of a negative band at 1228 cm^{-1} in Figure 5A (thick line) to 1210 cm^{-1} (Figure 5A, thin line) upon ^{13}C labeling of bicarbonate. The positive signal at 1257 cm^{-1} (Figure 5A, thick line) is only partly downshifted to 1252 cm^{-1} (Figure 5A, thin line) upon bicarbonate ^{13}C labeling. The ^{13}C sensitive component at 1258 cm^{-1} (Figure 5B) is assigned to a mode of bicarbonate in the Fe^{2+} state, while the main contribution at 1257 cm^{-1} that is insensitive to bicarbonate labeling is assigned to a protein mode.

In the 1700−1400-cm^{-1} region, numerous overlapping difference bands are observed in the Fe^{2+}/Fe^{3+} spectra (Figure 5A) that mask bicarbonate contributions. The ^{12}C *minus* ^{13}C spectrum of Figure 5B shows a broad positive band between 1600 and ≈1520 cm^{-1} and two negative bands at 1658 and 1495 cm^{-1}. Since the effect of ^{13}C labeling results in downshifts of bicarbonate bands, and since there is no positive counterpart at lower frequency for the negative band at 1495 cm^{-1} in the ^{12}C *minus* ^{13}C spectrum, this band is assigned to a mode of ^{13}C bicarbonate in the Fe^{2+} state. The corresponding mode of ^{12}C bicarbonate is expected between 1550 and 1520 cm^{-1}. The positive band at 1600−1520 cm^{-1} in Figure 5B can be decomposed into two broad components with maxima at 1600 ± 10 and 1530 ± 10 cm^{-1} which partly overlap around 1560 cm^{-1}. The band at 1530 ± 10 cm^{-1} is identified as the ^{12}C bicarbonate mode in the Fe^{2+} state which is downshifted to 1495 cm^{-1} upon ^{13}C labeling. The positive band at 1600 cm^{-1} can be interpreted as the downshift upon ^{13}C labeling of the negative signal at 1658 cm^{-1}. The signals at 1600 ± 10 cm^{-1} and 1658 cm^{-1} are therefore tentatively assigned to modes of ^{13}C- and ^{12}C-bicarbonate in the Fe^{3+} state, respectively. In this region, the attribution of the bicarbonate modes is complicated by overlap with strong differential signals of the protein in the individual Fe^{2+}/Fe^{3+} spectra. The minimum at 1658 cm^{-1} may not indicate the exact frequency position of the ^{12}C bicarbonate mode which is probably responsible for the small and broad negative band at 1658 ± 20 cm^{-1}.

The effect of $^1H/^2H$ exchange is displayed in Figure 6. The Fe^{2+}/Fe^{3+} spectra were obtained in ^2H_2O with ^{12}C- (thick line) and ^{13}C- (thin line) bicarbonate (Figure 6A). The spectra were normalized to the same absorbance change of ferrocyanide at 2040 cm^{-1} as in Figure 5A, and the ^{12}C *minus* ^{13}C spectrum is displayed in Figure 6B (solid line). Although the individual Fe^{2+}/Fe^{3+} spectra are different in H_2O and ^2H_2O, the comparison of the ^{12}C *minus* ^{13}C spectra in H_2O and ^2H_2O (Figure 6B, dashed and solid lines) reveals that only slight frequency shifts of bicarbonate modes are induced by $^1H/^2H$ exchange. In particular, the signals at 1348 and 1306 cm^{-1} and at 1244 and 1208 cm^{-1} in ^2H_2O correspond to the signals observed at 1339 and 1305 cm^{-1} and at 1230 and 1206 cm^{-1} in H_2O, respectively. Rather than slight

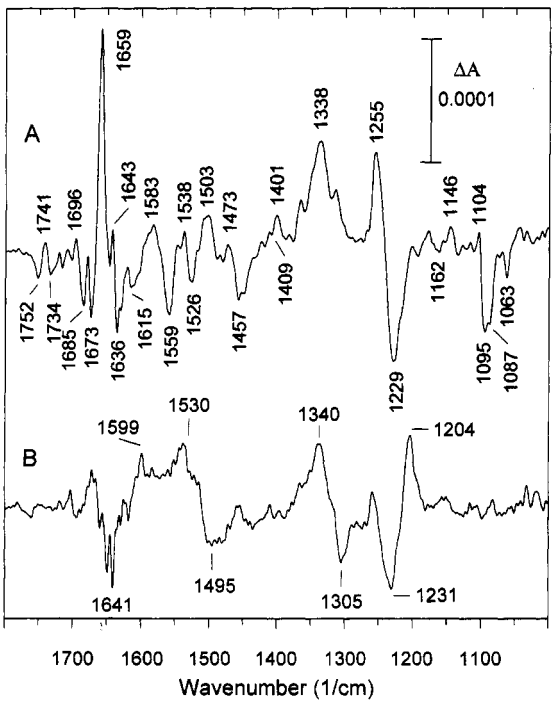

FIGURE 7: (A) Fe^{2+}/Fe^{3+} spectra obtained on ^{15}N labeled Tris-washed PS II membranes at pH 8. (B) ^{12}C *minus* ^{13}C spectrum; 4-cm^{-1} resolution, 4 °C, ≈120 000 scans.

frequency upshifts of these modes, the $^1H/^2H$ exchange results in a large change of band shape of the signals which is interpreted as the disappearence of a low-frequency component (see Discussion). The positive signal at 1263 cm^{-1} in Figure 6A is not modified upon ^{13}C labeling and exhibits a smaller amplitude as the corresponding signal at 1257 cm^{-1} in H_2O. Therefore, we conclude that the bicarbonate mode observed at 1258 cm^{-1} in H_2O (Figure 5B) disappears or is downshifted below 1000 cm^{-1} upon $^1H/^2H$ exchange, while the signal at 1263 cm^{-1} in ^2H_2O results from an upshift by 6 cm^{-1} of the 1257-cm^{-1} signal in H_2O. This upshift is in agreement with the attribution of this signal to the ν(CO) mode of a protonated tyrosine side chain (Dollinger et al., 1986).

The negative band at 1482 cm^{-1} and the positive one at 1530 cm^{-1} in Figure 6B (solid line) correspond to the signals of the ^{12}C *minus* ^{13}C spectrum in H_2O at 1530 ± 10 cm^{-1} and 1495 cm^{-1} and confirm their assignment to ^{12}C- and ^{13}C-bicarbonate modes of the Fe^{2+} state, respectively. Above 1550 cm^{-1}, differences are observed between the ^{12}C *minus* ^{13}C spectra in H_2O and ^2H_2O. This might be interpreted as an upshift upon $^1H/^2H$ exchange of the signals at 1658 ± 20/1600 ± 10 cm^{-1} in H_2O to 1686 ± 20/1632 ± 10 cm^{-1} in ^2H_2O, tentatively assigned to the $^{12}C/^{13}C$ bicarbonate modes in the Fe^{3+} state.

Figure 7A depicts the Fe^{2+}/Fe^{3+} spectrum obtained with ^{15}N-labeled PS II membranes in the presence of ^{12}C bicarbonate. The Fe^{2+}/Fe^{3+} spectrum was also obtained on PS II membranes in the presence of ^{13}C bicarbonate (not shown). The resulting ^{12}C *minus* ^{13}C spectrum is displayed in Figure 7B. Below 1400 cm^{-1}, the ^{12}C *minus* ^{13}C spectra obtained with ^{14}N- and ^{15}N-labeled membranes are almost identical. In particular, no effect of ^{15}N labeling is observed at 1380−1360 or 1120 cm^{-1}, where the ν(C−N) vibration of carbamates would occur (Davies & Roberts, 1992). In addition, the signals in the region from 1700−1400 cm^{-1} are also similar with ^{14}N- and ^{15}N-labeled membranes. Small differences at ≈1650 cm^{-1} cannot be rationalized by the formation of a carbamate species either in the Fe^{2+} or in the Fe^{3+} state and may be explained by the higher noise level in this region for spectra recorded with ^{15}N labeled membranes.

The Fe^{2+}/Fe^{3+} spectra also exhibit contributions from the protein backbone and from protein side chains modified by the iron reduction. Possible assignments can be proposed by the specific effects of $^1H/^2H$ exchange or of ^{15}N labeling on these modes. The largest effects of the $^1H/^2H$ exchange on the protein modes consist in smaller amplitudes of signals at 1673/1660 cm^{-1}, in the disappearance of the difference band at 1552/1539 cm^{-1}, and in the appearance of a strong negative signal at 1625 cm^{-1} in the Fe^{2+}/Fe^{3+} spectrum in ^2H_2O (Figure 6A). In this region, several absorption changes seem to overlap. However, the almost disappearance of the signal at 1552/1539 cm^{-1} in ^2H_2O is in agreement with its assignment to the ν(CN) + δ(NH) amide II mode of a peptide group. The negative signal at 1625 cm^{-1} in ^2H_2O could arise either from a glutamine, an asparagine, or an arginine side chain (Chirgadze et al., 1975). H_2O *minus* ^2H_2O double difference spectra (not shown) indicate that this signal could result from the downshift of a differential band at 1673/≈1660 cm^{-1} in H_2O to 1625/≈1610 cm^{-1} in ^2H_2O. The 1257-cm^{-1} band, upshifted to 1263 cm^{-1} upon $^1H/^2H$ exchange, is tentatively assigned to the ν(CO) mode of a protonated tyrosine side chain (Dollinger et al., 1986) and a positive signal at 1517 cm^{-1} to the corresponding ν(CC) mode of the tyrosine cycle. Small signals at 1753, 1742, 1732, and 1720 cm^{-1} in H_2O (Figure 5A) could arise from the ν(C=O) vibration of protonated aspartic or glutamic side chains (Venyaminov & Kalnin, 1990). The frequency shifts by at most 2 cm^{-1} observed for these bands upon $^1H/^2H$ exchange (Figure 6A) could indicate that these residues form strong hydrogen bonds [Maeda et al. (1992) and references therein] and/or are inaccessible to $^1H/^2H$ exchange. An effect of iron reduction on residues located at longer distances such as the 10a ν(C=O) ester mode(s) of the neutral intermediary electron acceptor pheophytin(s) (Nabedryk et al., 1990) cannot be excluded.

Two negative bands at 1094 and 1102 cm^{-1} and a positive one at 1111 cm^{-1} in Figure 3A are found at 1087, 1095, and 1104 cm^{-1}, respectively, in spectra obtained with ^{15}N-labeled PS II membranes (Figure 7A). The band shape of the signals is the same in the two spectra and the effect of ^{15}N labeling is interpreted as the downshift of these signals by 7 cm^{-1}. Two modes are observed at 1105 and 1086 cm^{-1} in IR spectra for neutral 4-methylimidazole (4-MeImH) and at 1097 and 1066 cm^{-1} for imidazole (ImH) [Berthomieu et al., 1992b; Majoube et al. (1995) and references therein]. Only the mode at 1086 cm^{-1} of 4-MeImH is affected upon $^1H_2O/^2H_2O$ exchange, which is not the case for the signals observed in PS II. Upon ^{15}N labeling of imidazole only one mode (at 1066 cm^{-1}) is downshifted by 7 cm^{-1} (Berthomieu et al., 1992b). This mode is almost insensitive to $^1H_2O/^2H_2O$ exchange (not shown). In PS II, the two negative signals observed at 1102 and 1094 cm^{-1} are downshifted upon ^{15}N labeling (Figure 5A). Therefore, we assign these modes observed in the Fe^{3+} state to histidine side chains having slightly different structures. In electrochemically induced oxidized *minus* reduced FTIR spectra of bis-4-MeImH complexes of iron protoporphyrin IX (Berthomieu

Table 1: Frequencies of Bicarbonate Modes in Model Compounds and PS II[a]

HCO_3	monomer[b]	dimer[c]	H_2O[d]	η^1 coord[e]	η^2 coord[f]	Fe^{2+} [d]	Fe^{3+} [d]
ν_{as} (CO)	1697 (−46)	1618	1648 (−62)	1634	1587	1530 ± 10 (−35)	*1658 ± 20 (−58)*
ν_s (CO)	1338 (−25)	1367	1363 (−22)	1353	1338	1338 (−29)	1228 (−18)
[+ δ (OH)]		[1405]					
$\nu_{as} - \nu_s$ (CO)	359 (−21)	251	285 (−40)	281	249	192 (−7)	*410 ± 20 (−20)*
$^2HCO_3$	monomer[b]	dimer[c]	H_2O[d]			Fe^{2+} [d]	Fe^{3+} [d]
ν_{as} (CO)	1687 (−46)	1615	1628			1530 ± 10 (−58)	*1686 ± 20 (−54)*
ν_s (CO)	1338 (−25)	1392	1366			1344 (−32)	1229 (−17)
[δ (OD)]		[1050]	[1037]			*[1041]*	
$\nu_{as} - \nu_s$ (CO)	349 (−21)	223	285			186 (−16)	*457 ± 20 (−43)*

[a] Data in parentheses represent the shifts induced by ^{13}C labeling of bicarbonate. Values in italics are tentative assignments. [b] Bernitt et al. (1965). [c] Nakamoto et al. (1965). [d] This work. [e] Crutcheley et al. (1977). [f] Yoshida et al. (1979).

et al., 1992b), a strong signal at 1103 cm^{-1} was assigned to a mode of the 4-MeImH ligand in the Fe^{3+}state by ligand substitution and isotope labeling. This mode was observed at 1099 cm^{-1} for the Fe^{3+}−4-methylimidazolate (4-MeIm$^-$) ligands at pH 12. Therefore, we propose that the signal at 1094 cm^{-1} in PS II could arise from the deprotonated side chain of a histidine ligand of the Fe^{3+} iron, while the signals at 1111/1102 cm^{-1} are proposed to arise from neutral histidine ligand(s). Positive signals at 1476 and 1150 cm^{-1} and a negative one at 1465 cm^{-1} in Figure 3A, downshifted to 1473, 1146, and 1457 cm^{-1}, respectively, upon ^{15}N labeling, are also tentatively assigned to histidine side-chain modes (Takeuchi et al., 1991). The 15-cm^{-1} downshift observed on the 1552/1539-cm^{-1} signal to 1538/1526 cm^{-1} (Figure 3A) for ^{15}N labeled membranes confirms the assignment to an amide II mode. Above 1620 cm^{-1}, predominant absorption of ν(C=O) modes masks the possible effect of ^{15}N labeling on amino acid side-chain modes. ^{14}N *minus* ^{15}N difference spectra in this region reveal a small differential signal at 1660 cm^{-1} and also small negative signals at 1677−1672 cm^{-1} and a positive one at 1636−1630 cm^{-1} (not shown). Other differences are also observed for the ^{14}N- and ^{15}N-labeled PS II membranes in the 1620−1580-cm^{-1} region and at 1503 cm^{-1} (Figure 7A). These signals could result from arginine and lysine side chains. The contribution of a lysine $\delta(NH_3^+)$ mode in the Fe^{3+} state is also suggested by the presence of negative signals at 1183 cm^{-1} in the Fe^{2+}/Fe^{3+}spectra in ^2H_2O that could correspond to the $\delta(ND_3^+)$ bending mode. Specific assignment of arginine and lysine residues will necessitate the study of mutants and of PS II with specifically labeled amino acids. Signals at 1409/1400 cm^{-1} and at 1561/1585 cm^{-1} (Figure 3A) are mostly insensitive to ^{15}N labeling and are tentatively assigned to the ν_s and ν_{as}(CO) vibrations of the carboxylate side chain of aspartate or glutamate. In addition, it cannot be excluded that the iron has a long-range charge effect on the neutral plastoquinone Q_A and that the difference band at 1643/1636 cm^{-1}, unaffected by either $^1H/^2H$ exchange or ^{15}N labeling, could be due to a slight downshift upon iron oxidation of the ν(C=O) mode of Q_A tentatively assigned at 1643 cm^{-1} (Berthomieu et al., 1990, 1992a) .

DISCUSSION

The metal−oxygen vibrations of metal−carbonate complexes are expected well below 1000 cm^{-1}. However, the possible coordination of bicarbonate to the non-heme iron of PS II can be determined since a correlation exists between the frequencies of carbonate and carboxylate observed between 1800 and 1000 cm^{-1} and their coordination to metals (Deacon & Phillips, 1980; Nakamoto, 1986).

The IR spectra of bicarbonate monomer ions determined by Bernitt et al. (1965) and Maguire and Rubalcava (1669) in various solid alkali halides show three normal modes in the 1800−1000-cm^{-1} region. The antisymmetric ν_{as}(CO) and symmetric ν_s(CO) stretching modes of the carboxylate group appear at 1697 and 1338 cm^{-1}, respectively, and the δ(COH) bending mode at 1211 cm^{-1}. These descriptions are approximate since, for each normal mode, vibrations from all atoms are actually involved. Upon ^{13}C labeling, frequency downshifts of 46 and 25 cm^{-1} are observed for the ν_{as}(CO) and ν_s(CO) modes of bicarbonate, respectively. Deuterated bicarbonate exhibits similar downshifts upon ^{13}C labeling. On the other hand, the δ(COH) mode is almost insensitive to ^{13}C labeling but is downshifted by ≈240 cm^{-1} upon deuteration (Bernitt et al., 1965; see also Table 1). In solution, hydrogen bonds are formed between bicarbonate molecules (dimeric complexes) or with water molecules. Spectra were recorded for ^{12}C bicarbonate in H_2O and ^2H_2O and for ^{13}C bicarbonate in H_2O [Figure 8; see also Davies and Oliver, (1972)]. The ν_{as}(CO) modes of ^{12}C bicarbonate and deuterated ^{12}C bicarbonate are observed at 1648 and 1628 cm^{-1} in H_2O and ^2H_2O, respectively. Hydrogen bonding results in a 40−50-cm^{-1} downshift of the ν_{as}(CO) mode. In dimers, stronger hydrogen bonds result in a downshift by ≈ 80 cm^{-1} of this mode (Novak et al., 1963; see also Table 1). Upon ^{13}C labeling, the ν_{as}(CO) mode is downshifted by ≈60 cm^{-1} (Figure 8B). In the presence of hydrogen bonds, the ν_s(CO) mode is coupled with the δ(OH) mode (Novak et al., 1963; Nakamoto et al., 1965) and the two modes give rise to overlapping absorbance bands in the region of the ν_s(CO) frequency. Upon deuteration, this coupling is cancelled and a δ(OD)- mode appears between 1080 and 1040 cm^{-1}. We therefore assign the small absorbance band at 1037 cm^{-1} in Figure 8C to the δ(OD) mode of deuterated bicarbonate in ^2H_2O which, as expected, does not shift significantly upon ^{13}C labeling (Table 1).

In PS II, the ^{13}C sensitive signals observed at 1530 ± 10 and 1338 cm^{-1} in the Fe^{2+} state can be assigned to the ν_{as} and ν_s(CO) modes of bicarbonate, respectively. $^1H/^2H$ exchange results in a change in shape and intensity of the ν_s(CO) mode at 1338 cm^{-1}, while bicarbonate ^{13}C isotope labeling influences only the frequency of this signal but not its band shape. Therefore, the δ(OH) mode appears to be coupled to the ν_s(CO) mode at 1338 cm^{-1} in the Fe^{2+} state as for bicarbonate in solution. Furthermore, a small positive band at 1041 cm^{-1} is observed in the Fe^{2+}/Fe^{3+} difference spectra obtained in ^2H_2O (Figure 6A) and this signal is

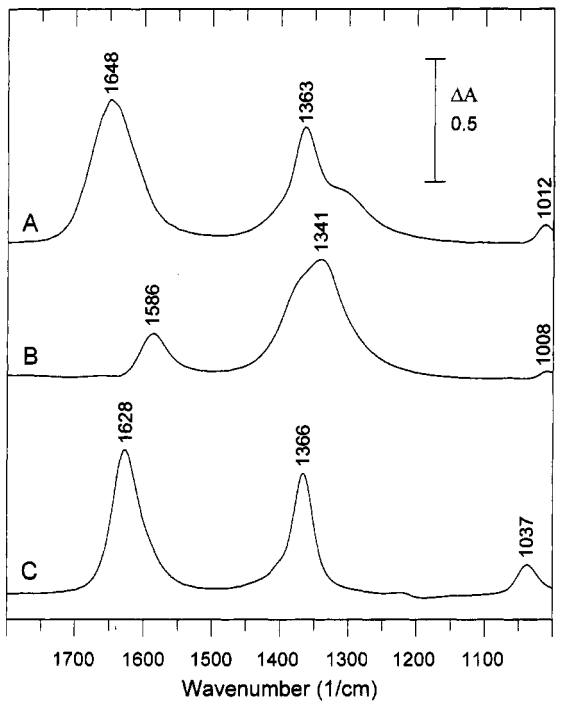

FIGURE 8: Absorption spectra of (A) ^{12}C bicarbonate and (B) ^{13}C bicarbonate in H_2O, and of (C) ^{12}C bicarbonate in ^2H_2O; contributions of H_2O and ^2H_2O have been subtracted after normalization at approximately 2140 and 1210 cm^{-1}, respectively; 20 °C, 100 mM concentration, 256 scans, 4-cm^{-1} resolution.

tentatively assigned to the δ(OD) mode of deuterated bicarbonate. The small signal at 1258 cm^{-1} that downshifts by 7 cm^{-1} upon bicarbonate ^{13}C labeling and that is absent or downshifted below 1000 cm^{-1} in ^2H_2O is tentatively assigned to the bicarbonate δ(COH) mode (Bernitt et al., 1965; Maguire & Rublacava, 1969). Thus the IR signals clearly indicate the binding of bicarbonate and not carbonate in the Fe^{2+} state. Furthermore, the observed coupling of the ν_s(CO) and δ(OH) modes is indicative for hydrogen bonding of bicarbonate with protein amino acids of PS II.

The frequency of the ν_{as}(CO) mode in PS II is significantly lower than for hydrogen-bonded bicarbonate compounds (Novak et al., 1963; Nakamoto et al., 1965; Bertoluzza et al., 1981). This frequency can only be rationalized by bicarbonate binding to the non-heme iron and is taken as experimental evidence that bicarbonate is a ligand of the iron. IR spectroscopy has been extensively used to determine the type of coordination in many carbonato-, formato-, bicarbonato-, and organic carboxylato-metal complexes [for reviews see Busca and Lorenzelli (1982) and Deacon and Phillips, (1980)]. Deacon and Phillips (1980) deduced a correlation between the frequencies of the ν_{as}(CO) and ν_s(CO) modes and the binding mode of the carboxylate group. Monodentate coordination removes the equivalence of the two oxygen atoms and results in a frequency increase of the ν_{as}(CO) mode and decrease of the ν_s(CO) mode as compared to the ionic form. Thus, the frequency difference between these modes [$\nu_{as}-\nu_s$ (CO)] is substantially larger than in the ionic form. On the contrary, bidentate ligation is clearly indicated if $\nu_{as}-\nu_s$(CO) is significantly smaller. If the difference is close to that of the ionic form, both binding modes are possible. These criteria were determined independently from the nature and charge of the metal ion and its other ligands. The structures of two bicarbonato complexes have been reported with either monodentate (Crutchley et al., 1977) or bidentate (Yoshida et al., 1979) ligation. The ν_{as}(CO) and ν_s(CO) frequencies of bicarbonate in these complexes (Table 1) show that the correlation established for organic carboxylato-metal complexes can be applicated for determining the bicarbonate binding mode [see also Busca & Lorenzelli, (1982)]. In PS II, the $\nu_{as}-\nu_s$(CO) difference of 192 cm^{-1} found for the Fe^{2+} state is significantly smaller than for hydrogen-bonded ionic bicarbonate (251 cm^{-1}) and indicates unambiguously bidentate ligation to the non-heme iron (Fe^{2+}).

In the Fe^{3+} state, the band at 1228 cm^{-1}, downshifted by 18 cm^{-1} upon ^{13}C labeling, exhibits a similar behavior upon $^1H/^2H$ exchange as the ν_s(CO) mode at 1338 cm^{-1} of bicarbonate in the Fe^{2+} state. Both signals are therefore assigned to the same mode, downshifted by 110 cm^{-1} upon iron oxidation. In the Fe^{3+} state, the ν_{as}(CO) mode is not identified with certainty but is estimated at 1658 ± 20 cm^{-1} for ^{12}C bicarbonate and at 1600 ±20 cm^{-1} for ^{13}C bicarbonate. Iron oxidation thus causes an upshift of this mode by ≈100 cm^{-1}. Consequently, $\nu_{as}-\nu_s$(CO) is strongly enhanced to 430 ± 20 cm^{-1} in the Fe^{3+} state. Increasing charge on the metal is expected to modify the bicarbonate vibrations. In carbonato-bridged cobalt(II) complexes, up- and downshifts by 60−80 cm^{-1} were observed for the ν_{as} and ν_s(CO) IR modes of carbonate upon metal oxidation (Harada et al., 1991). According to the relationship between the metal polarizing power and $\nu_{as}-\nu_s$(CO) established by Jovilet et al. (1982) for carbonato complexes, we estimate that iron oxidation could result in an increase of $\nu_{as}-\nu_s$(CO) by about 100 cm^{-1}. It seems therefore unlikely that the enhancement by 240 ± 20 cm^{-1} of $\nu_{as}-\nu_s$(CO) in PS II upon iron oxidation only results from the increased charge on the iron. The large difference is best explained by monodentate coordination of bicarbonate to the oxidized non-heme iron. An alternative interpretation is the assignment to a bidentate hydrogen-bonded carbonate ligand (Fujita et al., 1962). The sensitivity of the 1229-cm^{-1} signal to deuteration, i.e., intensity change rather than frequency shift, favors, however, its assignment to the bicarbonate ν_s(CO) mode. Therefore, we propose that bicarbonate is a monodentate ligand of the Fe^{3+} iron. Recently, Darensbourg et al. (1993) and Looney et al. (1993) have assigned bands at 1647 and 1675 cm^{-1} and at 1312 and 1302 cm^{-1} in metal−bicarbonato complexes to the ν_{as}(CO) and ν_s(CO) modes of bicarbonate, respectively, and also proposed monodentate binding.

Upon $^1H/^2H$ exchange, the ν_{as}(CO) mode of bicarbonate in solution downshifts by 20 cm^{-1}. This shift is strongly dependent on the hydrogen bonding of bicarbonate since it is very small for the dimeric form (Table 1). In PS II, no significant change is observed for the bicarbonate ν_{as}(CO) mode in the Fe^{2+} state, and an upshift is indicated for the Fe^{3+} state. These observations suggest strong hydrogen bonding of the bicarbonate oxygens with protein residues or water molecules.

Bidentate binding of bicarbonate to the Fe^{2+} iron is in agreement with the close analogy found between the Mössbauer spectra of the iron in PS II and in the bacterial RC (Petrouleas et al., 1987). Heterogeneity of the iron binding sites was evoked from Mössbauer spectroscopy (Petrouleas et al., 1992) and from the two forms of the iron−semiquinone EPR signals at $g = 1.82$ and $g = 1.9$ (Rutherford & Zimmermann, 1984). It was proposed that this heterogeneity would correspond to a fraction of PS II centers where the

iron has a very high midpoint potential [reviewed in Diner et al. (1991)]. In this study, we obtain IR signals only from iron centers that can be oxidized by ferricyanide. The three-dimensional structure of Cu(II)-reconstituted lactoferrin showed that one metal-binding site contains a monodentate bicarbonate ligand (Shongwe et al., 1992). The comparison of metal centers with bidentate carbonate and monodentate bicarbonate ligands shows that the change in coordination is easily achieved by a slight rotation of the (bi)carbonate almost in its own plane, while the overall structure of the protein is conserved. In PS II, a similar rotation upon iron oxidation will slightly modify bicarbonate interactions with protein polar groups. Several IR signals from amino acid residues and side chains contribute to the Fe^{2+}/Fe^{3+} spectra. Signals are tentatively assigned to peptide NH group(s) as well as to a tyrosine and an aspartate or glutamate side chains that could participate in the hydrogen-bond network around the bicarbonate.

In the presence of *o*-phenanthroline or DCMU at alkaline pH or in dried PS II membranes, the EPR signal of the Fe^{3+} iron is modifed and an axial EPR signal with $g_{xyz} = 6$ is observed for a fraction of the oxidized iron (Itoh et al., 1986; Diner et al., 1987; Deligiannakis et al., 1992). Orientation dependence of this Fe^{3+} EPR signal and comparison with bacterial RC indicated the existence of a pseudo-C_3 symmetry of the iron ligands in the vertical plane of the membrane formed by the bicarbonate oxygen(s) and the nitrogens of the two histidines also hydrogen-bonded to Q_A and Q_B. This pseudosymmetry would be achieved by a slight rotation of the bicarbonate oxygen ligand to form angles of about 120° with the two histidine nitrogens. This model suggests that only five ligands coordinate the Fe^{3+} iron, giving the axial $g = 6$ EPR signal. For centers with the more rhombic EPR signal, the presence of a sixth ligand, a protein residue or a water molecule, cannot be excluded. For Cu-reconstituted lactoferrin, only five ligands are found for the Cu(II) site where bicarbonate is a monodentate ligand (Shongwe et al., 1992). The structure is stabilized by hydrogen bonding between the bicarbonate hydroxyl group and the oxygen of the tyrosine ligand. A similar model can be proposed for PS II. Signals at $g = 8.05$ and $g = 5.6$ would correspond to PS II centers where a hydrogen bond between bicarbonate and a histidine ligand reduces the rotation of bicarbonate upon iron oxidation as compared to centers giving the $g = 6$ EPR signal. The presence of *o*-phenanthroline or perturbation of the hydrogen-bond network in dehydrated samples would suppress this hydrogen bond, leading to the larger displacement of the bicarbonate oxygen ligand. From the FTIR spectrum, the absence of a clear negative signal at 1390−1365 cm^{-1} seems to rule out the possible contribution of the ν_s(CO) mode of a monodentate aspartate or glutamate ligand for the Fe^{3+} iron [Noguchi et al. (1995b) and references therein]. The presence of a sixth putative ligand in the Fe^{3+} state will be studied by comparison of Fe^{2+}/Fe^{3+} spectra obtained in the absence or presence of *o*-phenanthroline.

The midpoint potential of the iron is pH-dependent with −60 mV/pH unit in the pH 5.5−8 range (Bowes et al., 1979; Wraight, 1985). Therefore, proton release occurs upon iron oxidation. We interpret the IR data as indicating that bicarbonate does not deprotonate upon iron oxidation. We propose that the negative signal at 1094 cm^{-1} corresponds to the side chain of one histidine ligand of the iron that deprotonates in the Fe^{3+} state. The influence on the EPR spectrum of the Fe^{3+} iron of quinone inhibitors in the Q_B site and notably of *o*-phenanthroline (Diner & Petrouleas, 1987b) and also the possible oxidation of the iron by the semiquinone form of high-potential quinones like *p*-phenylbenzoquinone (Zimmermann & Rutherford, 1986) suggest that the histidine hydrogen-bonded to Q_B (D1-His215) could deprotonate. The deprotonation of the histidine could determine the pH dependence of the iron midpoint potential. More complex regulation must be involved if the protein or a water molecule provides a sixth ligand to the oxidized iron.

CONCLUSION

From the FTIR results presented in this work, we conclude that bicarbonate is a bidentate ligand of the non-heme iron in PS II like M-Glu232 in the bacterial RCs. We further propose that upon iron oxidation bicarbonate becomes a monodentate ligand and that iron oxidation is accompanied by the deprotonation of one histidine ligand. The presence of a sixth ligand in the Fe^{3+} state, and also a precise characterization of the various amino acid residues and side chains involved in bicarbonate binding, will be investigated after bicarbonate replacement with other carboxylate anions and in selectively labeled PS II membranes.

ACKNOWLEDGMENT

We gratefully acknowledge A. Boussac for the kind gift of ^{15}N labeled PS II membranes and also for useful discussions and help with EPR experiments, V. Petrouleas and Y. Deligiannakis for interesting discussions, and J. Breton and E. Nabedryk for careful reading of the manuscript. R.H. was supported by an EMBO fellowship.

REFERENCES

Allen, J. P., Feher, G., Yeates, T. O., Kommiya, H., & Rees, D. C. (1988) *Proc. Natl. Acad. Sci. U.S.A. 85*, 8487−8491.

Babcock, G. T.; & Sauer, K. (1973) *Biochim. Biophys. Acta 325*, 483−503.

Babcock, G. T.; & Sauer, K. (1975) *Biochim. Biophys. Acta 376*, 329−344.

Barry, B. A., & Babcock, G. T. (1987) *Proc. Natl. Acad. Sci. U.S.A. 84*, 7099−7103.

Bauscher, M., Nabedryk, E., Bagley, K., Breton, J., & Mäntele, W. (1990) *FEBS Lett. 261*, 191−195.

Bernitt, D. L., Hartman, K. O., & Hisatsune, I. C. (1965) *J. Chem. Phys. 42*, 3553−3558.

Berthold, D. A., Babcock, G. T., & Yocum, F. (1981) *FEBS Lett. 61*, 231−234.

Berthomieu, C., Nabedryk, E., Mäntele, W., & Breton, J. (1990) *FEBS Lett. 269*, 363−367.

Berthomieu, C., Nabedryk, E., Breton, J., & Boussac, A. (1992a) in *Research in Photosynthesis* (Murata, N., Ed.) Vol. II, pp 53−56, Kluwer Academic Publishers, Dordrecht, The Netherlands.

Berthomieu, C., Boussac, A., Mäntele, W., Breton, J., & Nabedryk, E. (1992b) *Biochemistry 31*, 11460−11471.

Bertoluzza, A., Monti, P., Morelli, M. A., & Battaglia, M. A. (1981) *J. Mol. Struct. 73*, 19−29.

Blubaugh, D. J., & Govindjee (1988) *Photosynth. Res. 19*, 85−128.

Bowes, J. M., Crofts, A. R., & Itoh, S. (1979) *Biochim. Biophys. Acta 547*, 320−335.

Breton, J., Berthomieu, C., Thibodeau, D. L., & Nabedryk, E. (1991) *FEBS Lett. 288*, 109−113.

Busca, G., & Lorenzelli, V. (1982) *Mater. Chem. 7*, 89−126.

Cao, J., Vermaas, W. F. J., & Govindjee (1991) *Biochim. Biophys. Acta 1059*, 171−180.

Chirgadze, Y. N., Federov, O. V., & Trushina, N. P. (1975) *Biopolymers 14*, 679−694.
Cordes, N. D., & Walter, C. S. C. (1968) *Spectrochim. Acta 24A*, 237−252.
Crutcheley, R. J., Powell, J., Faggiani, R., & Lock, C. J. L. (1977) *Inorg. Chim. Acta 24*, L15−L16.
Davies, A. R., & Oliver, B. G. (1972) *J. Solution Chem. 1*, 329−335.
Davies, P. R., & Roberts, M. W. (1992) *J. Chem. Soc., Faraday Trans. 88*, 361−368.
Darensbourg, D. J., Meckfessel, M. L., & Reibenspies, J. H. (1993) *Inorg. Chem. 32*, 4675−4675
Deacon, G. B., & Phillips, R. J. (1980) *Coord. Chem. Rev. 33*, 227−250.
Deisenhofer, J., & Michel, H. (1989) *EMBO J. 8*, 2149−2169.
Dekker, J. P., van Gorkom, H. J., Brok, M., & Ouwehand, L. (1984) *Biochim. Biophys. Acta 764*, 301−309.
Deligiannakis, Y., Tsekos, N., Petrouleas, V., & Diner, B. A. (1992) *Biochim. Biophys. Acta 1140*, 260−270.
Deligiannakis, Y., Petrouleas, V., & Diner, B. A. (1994) *Biochim. Biophys. Acta 1188*, 260−270.
Diner, B. A., & Petrouleas, V. (1987a) *Biochim. Biophys. Acta 895*, 107−125.
Diner, B. A., & Petrouleas, V. (1987b) *Biochim. Biophys. Acta 893*, 138−148.
Diner, B. A., & Petrouleas, V. (1990) *Biochim. Biophys. Acta 1015*, 141−149.
Diner, B. A., Petrouleas, V., & Wendoloski, J. J. (1991) *Physiol. Plant. 81*, 423−436.
Dollinger, G., Eisenstein, L., & Lin, S.-L. (1986) *Biochemistry 25*, 6524−6533.
Eaton-Rye, J. J., & Govindjee (1988) *Biochim. Biophys. Acta 935*, 237−257.
Ford, R. C., & Evans, M. C. W. (1983) *FEBS Lett. 160*, 159−164.
Fujita, J., Martell, A. E., & Nakamoto, K. (1962) *J. Chem. Phys.* 36, 339−344.
Govindjee, & Van Rensen, J. J. S. (1993) in *The Photosynthetic Reaction Center* (Deisenhofer, J., & Norris, J. R., Eds.) Vol. I, pp 357−389, Academic Press, San Diego, CA.
Harada, H., Kodera, M., Vuckovic, G., Matsumoto, N., & Kida, S. (1991) *Inorg. Chem. 30*, 1190−1194.
Hienerwadel, R., Boussac, A., & Berthomieu, C. (1993a) in *Fifth International Conference of the Spectroscopy of Biological Molecules* (Theophanides, T., Anastassopopoulou, J., & Fotopoulos, N., Eds.) pp 317−318, Kluwer Academic Publishers, Dordrecht, The Netherlands.
Hienerwadel, R. (1993b) Ph.D. Thesis, Department of Chemistry, University of Freiburg, Germany.
Ikegami, I., & Katoh, S. (1973) *Plant Cell Physiol. 14*, 829−836.
Itoh, S., Tang, X. S., & Satoh, K. (1986) *FEBS Lett. 205*, 275−281.
Jovilet, J. P., Thomas, Y., Taravel, B., Lorenzelli, V., & Busca, G. (1982) *J. Mol. Struct. 79*, 403−408.
Looney, A., Han, R., McNeill, K., & Parkin, G. (1993) *J. Am. Chem. Soc. 115*, 4690−4697.
Maeda, A., Sasaki, J., Shichida,Y., Yoshizawa, J., Hang, M., Ni, B., Needleman, R., & Lanyi, J. (1992) *Biochemistry 31*, 4684−4690.
Maguire, P. M., & Rubalcava, H. E. (1669) *Inorg. Chem. 8*, 246−251.
Majoube, M., Millié, Ph., & Vergoten, G. (1995) *J. Mol. Struct. 344*, 21−36.
Mäntele, W. (1993) *Trends Biochem. Sci. 18*, 197−202.
Michel, H., & Deisenhofer, J. (1988) *Biochemistry 27*, 1−7.
Nabedryk, E., Andrianambinintsoa, S., Berger, G., Leonhard, M., Mäntele, W., & Breton, J. (1990) *Biochim. Biophys. Acta 1016*, 49−54.
Nakamoto, K., Sarma, Y. A., & Ogoshi, H. (1965) *J. Chem. Phys. 43*, 1177−1181.
Nakamoto, K. (1986) *Infrared and Raman Spectra of Inorganic and Coordination Compounds*, 4rd ed., Wiley, New York.
Noguchi, T., & Inoue, Y. (1995a) *J. Biochem. (Tokyo) 118*, 9−12.
Noguchi, T., Ono, T., & Inoue, Y. (1995b) *Biochim. Biophys. Acta 1228*, 189−200.
Novak, A., Saumagne, P., & Bok, L. D. C. (1963) *J. Chim. Phys. 60*, 1385−1395.
Petrouleas, V., & Diner, B. A. (1986) *Biochim. Biophys. Acta 849*, 264−275.
Petrouleas, V., & Diner, B. A. (1987) *Biochim. Biophys. Acta 893*, 126−137.
Petrouleas, V., & Diner, B. A. (1990) *Biochim. Biophys. Acta 1015*, 131−140.
Petrouleas, V., Sanakis, Y., Deligiannakis, Y., & Dinar, B. A. (1992) in *Research in Photosynthesis* (Murata, N., Ed.) Vol II., pp 119−122, Kluwer Academic Publishers, Dordrecht, The Netherlands.
Petrouleas, V., Deligiannakis, Y., & Diner, B. A. (1994) *Biochim. Biophys. Acta 1188*, 260−270.
Rutherford, A. W., & Zimmermann, J.-L. (1984) *Biochim. Biophys. Acta 767*, 168−175.
Shongwe, M. S., Smith, C. A., Ainscough, E. W., Baker, H. M., Brodie, A. M., & Baker, E. N. (1992) *Biochemistry 31*, 4451−4458.
Stemler, A., & Murphy, J. B. (1985) *Plant Physiol. 77*, 974−977.
Takeuchi, H., Kimura, Y., Koitabasdhi, I., & Harada, I. (1991) *J. Raman Spectrosc. 22*, 233−236.
Trebst, A. (1986) *Z. Naturforsch. 41C*, 240−245.
Venyaminov, S. Y., & Kalnin, N. N. (1990) *Biopolymers 30*, 1243−1257.
Vermaas, W. F. J., & Rutherford, A. W. (1984) *FEBS Lett. 175*, 243−248.
Vermaas, W. F., Van Rensen, J. J. S., & Govindjee (1982) *Biochim. Biophys. Acta 681*, 242−247.
Wraight, C. A. (1985) *Biochim. Biophys. Acta 809*, 320−330.
Wydrzynski, T., & Govindjee (1975) *Biochim. Biophys. Acta 387*, 403−408.
Yoshida, T., Thorn, D. L., Okano, T., Ibers, J. A., & Otsuka, S. (1979) *J. Am. Chem. Soc. 18*, 412−421.
Zimmermann, J.-L., & Rutherford, A. W. (1986) *Biochim. Biophys. Acta 851*, 416−423.
Zimmermann, J.-L., Boussac, A., & Rutherford, A. W. (1993) *Biochemistry 32*, 4831−4841.

BI951952Y